Structural and Regenerative Aspects of the Hydra Head Activator Neuropeptide in the Newt, *Notophthalmus viridescens*

Thesis

Submitted to

The College of Arts and Sciences of the

UNIVERSITY OF DAYTON

In Partial Fulfillment of the Requirements for

The Degree

Master of Science in Biology

by

Ernesto Jorge Fuentes

UNIVERSITY OF DAYTON

Dayton, Ohio

December, 1992

Structural and Regenerative Aspects of the Hydra Head Activator Neuropeptide in the Newt, *Notophthalmus viridescens*

APPROVED BY:

Dr. Panagiotis A. Tsonis
(Advisor)

Dr. Mary Jo Vesper
(Faculty Reader)

Dr. Kenneth J. McDougall
(Faculty Reader)

Dr. John J. Rowe
(Department Chairman)

ABSTRACT

Title: Structural and Regenerative Aspects of the Hydra Head Activator Neuropeptide in the Newt, *Notophthalmus viridescens*

Name: Fuentes, Ernesto Jorge
University of Dayton, 1992

Advisor: Dr. P.A. Tsonis

The hydra head activator (HHA) neuropeptide was first isolated from the freshwater *Cnidaria, Hydra vulgaris* (formerly *Hydra attenuata*). Subsequent studies have revealed its presence and conserved sequence (NH_2-pGlu-P-P-G-G-S-K-V-I-L-F-COOH) in many species including mammals. In regenerating hydra, the peptide influences head-specific differentiation of epithelial cells and acts as a mitogen. In this study, the presence of the HHA peptide and its influence on regenerating newt limbs (*Notophthalmus viridescens*) was investigated. Immunohistological analysis localized the HHA peptide in the adult newt brain, eye, intestine, and regenerating blastema.

Nine-day limb regenerates were completely denervated by transecting the brachial nerves. The following day, HHA-soaked beads were implanted into the blastema under the wound epithelium and regeneration was studied for two weeks. Results suggest a slight progression in blastema growth occurred compared to denervated controls.

The structure of the HHA neuropeptide has been previously studied using NMR, CD, and Raman spectroscopy and determined to contain between 62-67% anti-parallel β-pleated sheet, and predicted to assume a β-turn near the amino terminus. We have utilized spectroscopic data with the Double-Iterated Kalman Filter (DIKF) technique and CHARMm molecular mechanics to produce a molecular model of the HHA peptide. Consistent with the secondary structure prediction, an anti-parallel β-pleated sheet topology was evident from the serine amino acid to the carboxyl terminus. Additionally, a β-turn occurred near the amino carboxyl terminus. Results indicate that fluctuations occurring at both termini may serve to stabilize the structure ultimately allowing the amino terminus access to its receptor protein.

ACKNOWLEDGEMENT

Throughout the course of my studies I have been very fortunate to interact with many people at the University of Dayton and elsewhere. Each person has contributed to me professionally and personally, and I wish to thank them here. Specifically, I with to thank Dr. P.A. Tsonis and all the members of the Tsonis lab for all their help, guidance, and patience. A special thank you is extended to Dr. Ruth Pachter and all those at the Materials Laboratory at Wright-Patterson Air Force Base. Finally, to my parents and sisters I am eternally grateful for their love and support, which without none of this would have been possible.

TABLE OF CONTENTS

LIST OF FIGURES

LIST OF TABLES

CHAPTER 1.

Review of Literature

The study of regenerative processes offers insight into the regulation and maintenance of cellular growth and differentiation. Since the pioneering investigations of Trembley (1740), Spallanzani (1769) and numerous others, regeneration of tissues and organs has been documented in many organisms such as hydra, killfish, catfish, salamanders, and mammals (Goss, 1969). In mammals, regeneration is limited, while urodele (tailed) amphibians and the cnidarian hydra have been studied extensively for their broad regenerative capabilities (Ord & Stocken, 1984).

In 1769, Spallanzani was the first to report on the regenerative potential of salamanders. In his account, Spallanzani describes the phenomena of tail and limb regeneration in several species (Spallanzani, 1769). Today, the urodele amphibians such as the newt (*Notopthalmus viridescens*) and the axolotl (*Ambystoma mexicanum*), the only vertebrates that are able to undergo regeneration as adults, have become model systems for the study of regeneration phenomenon and limb pattern formation.

An urodele amphibian can regenerate an experimentally amputated limb at any level on the proximal-to-distal axis (shoulder to fingertip) beginning at the plane of amputation (reviewed by Stocum, 1984). Upon amputation of the limb, wound healing begins by the migration of epidermal cells to the amputation plane, forming the wound epidermis. These epidermal cells accumulate at the wound site yielding a thickened apical epidermal cap. Mesodermal cells, such as cartilage and muscle, beneath the epidermal cap dedifferentiate to unspecific, embryonic-like cells resulting in an apical bud termed blastema. The blastema enlarges due to cellular

proliferation, redifferentiates, and undergoes pattern specification. The final stages of limb regeneration involve morphogenesis whereby the limb stump extends distally with concomitant formation of any missing digits (Goss, 1969; Stocum, 1984; Tsonis, 1991). Detailed morphological accounts and specific staging systems for limb regeneration have been published elsewhere and will not be discussed here (Iten and Bryant, 1973; Tank et al., 1976; Washabaugh and Tsonis, 1991).

The limb regeneration process is inextricably dependent upon the formation of an epithelial wound covering, adequate innervation (presence of nerves), blastema cells, and appropriate chemical "factors" (Liversage 1987; Tsonis 1991). The apical epithelial covering provides protection, positional cues and patterning information. The importance of the wound epithelium is underscored by the failure of limbs to regenerate when the epidermal cap is UV-irradiated or completely removed (reviewed by Stocum, 1985).

An adequately innervated limb will regenerate normally while denervation prevents or delays the formation of a limb regenerate (reviewed by Singer, 1952). Singer's "nerve threshold" theory postulates that nerves provide a trophic or neurotrophic influence on the blastema only when sufficient innervation is present. Therefore, below some particular threshold of nerves, neurotrophic activity ceases and regeneration is inhibited. Specifically, denervation has been reported to affect the blastema cell cycle at the G_1 (Maden, 1978 and 1979) and G_2 stages (Tassava, 1978). Moreover, denervated limbs have reduced DNA and protein synthesis which

can be partially rescued by the infusion of nerve extracts (Lebowitz and Singer, 1970; Jabaily and Singer, 1977).

The local chemical environment surrounding the regenrating limb seems to be crucial. Liversage (1985) proposes the "hormonal milieu" concept which implies that a sufficient and specific quantity of hormonal background is necessary for regeneration to proceed. This point is emphasized by the inhibition of regeneration upon hypophysectomy (Liversage and Globus, 1977; Liversage et al., 1985).

The process of limb regeneration is one of specific cellular responses to trophic, mitogenic, and morphogenic factors (Brockes, 1984; Liversage, 1987). These factors act at the cellular level and control specific aspects of cell differentiation and proliferation. These factors include retinoids, growth factors, and peptide hormones.

Retinoids

The retinoids are a class of compound containing a hydrocarbon ring and an attached conjugated hydrocarbon chain whose terminus is polar. These compounds are synthesized in animals from plant carotenoids. A representative member of these compounds is Vitamin A (retinol) which is synthesized and stored in the liver and released to tissues via the circulatory system. Once in the tissues, retinol is carboxylated and the resulting product termed retinoic acid (Blomhoff et al., 1990).

Retinoic acid (RA) seems to have two major functions. RA appears to be involved in epithelial cell differentiation and is intimately involved in the positional memory of regenerating and developing cells (reviewed by Brockes, 1989). In

regenerating urodele limbs, the blastema is "proximalized" due to RA. The positional memory of the cells is altered and the blastema behaves as though it were derived from a more proximal location (Thomas & Stocum, 1984; Maden, 1982). These effects are dose and time-dependent and most pronounced when administered early in blastema formation (Maden et al., 1985).

The urodele limb with RA has become an widely used experimental system for limb developmental and regeneration studies. The action of RA has been proposed to be mediated via a receptor-ligand complex analogous to steroid-hormone complexes. In the current model, the hormone binds to the monomeric receptor inducing translocation to the nucleus and/or receptor dimerization. The dimer then binds to its target DNA response element which influences transcriptional events (Beato, 1989; Evans, 1988). Recently, a gene was isolated (RARα) that shares homology with the steroid hormone receptor superfamily and codes for a protein that binds retinoic acid (Giguere et al., 1987; Petkovich et al., 1987). Giguere et al. (1989) have investigated the spatial expression of the RARα gene in blastema tissue and found no significant differences along the proximal-to-distal axis as one might expect for a morphogen that alters positional memory. To date several other retinoic acid receptors have been isolated leading to the designations of RARα, RARβ, RARγ, and RXRα (Blomhoff, 1990). Evidence now suggests that these receptors may form dimers among themselves and/or with other steroid receptors (thyroid hormone and vitamin D_3 receptors) adding an additional level of complexity to their mode of action (Bugge et al., 1992). In addition to the nuclear RAR, cytoplasmic retinoic and retinol

binding proteins (CRABP and CRBP) have been isolated (Blomhoff, 1990). Their function is elusive, however, there is speculation that they may act to sequester RA and retinol for later use by the cell.

Growth factors

Several growth factors have been associated with neurotrophic and mitogenic events. Most noteworthy are the fibroblast (Carlone and Mescher, 1985) and glilial (Brockes & Kintner, 1986) growth factors. The fibroblast growth factor (FGF) has been isolated from the brain and pituitary by several laboratories (Gospodarowicz, 1974; Westall et al., 1978). In each case that mitogenic activity was found, however, there remain discrepancies between the chemical characterization of each isolate. The mitogenic activity of FGF was initially found in fibroblasts and since then a proliferative effect has been noticed on newt regenerating blastema (Mescher & Loh, 1981).

The glial growth factor (GGF), a true neuromitogen, was first identified by its mitotic activity on rat Schwann cells - cells which notoriously lack response to mitogens (Raff et al., 1978). The GGF is a basic protein with an apparent molecular weight of 31,000 daltons. In urodele amphibians it is present in nervous and blastemal tissue but upon denervation is no longer detectable (Brockes & Kintner, 1986). Furthermore, GGF was responsible for the induction of mitosis as seen through an increased thymidine labelling index.

Peptides

Although most studies concerning mitotic factors have centered on proteins, recent studies have shown that neuropeptides and peptide hormones may also possess mitotic activity (Globus & Alles, 1990). Bombesin was first isolated from frog skin and is known to elicit the release of a host of other peptides including insulin and prolactin (Rozengurt & Sinnett-Smith, 1983). Rozengurt and Sinnett-Smith were able to show that bombesin is a potent mitogen on 3T3 cells and works synergistically with insulin. Recently, Globus and Alles (1990) have purportedly detected members of the tachykinin family (eledoisin, kassinin, substance K and neuromedin K) and the non-tachykinin bombesin and met-enkelphalin in newt brain and spinal cord, however their localization in the blastema was not well defined.

In the same study, substance P (SP) was successfully localized and characterized in the blastema. It was predominately distributed along the periphery of epidermal cells while the basal germinative epidermal layer remained unreactive. In further experiments, the intensity of SP antisera reaction was found to correlate with the expected density of innervation in the epidermis. Previously, it was shown that SP behaves as a mitogen in cultured blastema cells and its action could be suppressed by the inclusion of anti-SP in the culture (Globus et al., 1983). Together, this data suggests a possible link between the localization of SP and its mitogenic effect on the blastula. Possibly, its role is to act on epidermal cells which in turn release factors which are responsible for the observed mitotic effect. Triparte control of limb regeneration was proposed by Globus (1978). In this model, nerves, the

apical epidermal cap, and insulin are essential for limb regeneration. Subsequent studies revealed insulin to be a potent promoter of cultured blastema cells (Vethamany-Globus, 1987). From *in vivo* experiments, somatostatin, a known inhibitor of insulin release, was suggested to be responsible for the inhibition of limb regeneration (Vethamany-Globus, 1987).

The hydra head activator (HHA) neuropeptide, as the name implies, was first recognized in the freshwater *Cnidaria, Hydra attenuata*. Subsequent studies have revealed its conserved presence through many species including mammals (Bodenmüller and Schaller, 1981). In hydra, the head activator neuropeptide functions as a growth and differentiation factor. In a dose dependent fashion, the neuropeptide is mitogenic to all cell types arrested at the G_2 transition. As a differentiation factor, the HHA neuropeptide targets epithelial and interstitial stem cells. These cells, once stimulated by the HHA neuropeptide will differentiate to head- specific ectodermal, endodermal, or neural cells.

In addition to HHA's conserved sequence, there is evidence that the growth-controlling function of the peptide may also be preserved. The HHA has been isolated from the human hypothalamus and brain tissues of several other mammalian species (Bodenmüller & Schaller, 1981). In developing rat embryos, the expression of HHA appears early and lasts throughout development (Schaller et al., 1989a). Furthermore, HHA is also present in tumors and tumor cell lines of neural and endocrine origin (Schaller, 1985). One particular study suggests that the HHA

peptide acts as an autocrine growth factor at the G_2/mitosis transition of a neuroblastoma cell line (Schaller et al., 1989b).

Interestingly, the activity of the HHA in other commonly used regenerative model organisms has not been reported in the literature. In amphibian urodeles, it seems to be a logical candidate as a neuromitogen - it originates in neural tissue and possesses mitogenic activity.

The essential role of nerve cells seems to be linked to the several growth and stimulatory factors they produce and subsequently release. Other chemical factors such as peptide hormones and retinoids also seem to play a crucial role in regeneration. These factors have been implicated in the induction of mitosis and morphogenesis and hence are considered mitogenic and morphogenic factors. Additionally, the formation of chemical gradients for differential expression of these factors may be the final influencing determinant for the sustained progression of development and regeneration.

Literature Cited

Beato, M. (1989). Gene regulation by steroid hormones. *Cell* **56:** 335-344.

Blomhoff, R., Green, M.H., Berg, T. and Norum, K.R. (1990). Transport and storage of Vitamin A. *Science* **250:** 399-404.

Bodenmüller, H. and Schaller, H.C. (1981). Conserved amino acid sequence of a neuropeptide, the activator, from coelenterates to humans. *Nature* **293**: 579-580.

Brockes, J.P. (1984). Mitogenic growth factors and nerve dependence on limb regeneration. *Science* **225:** 1280-1287.

Brockes, J.P. and Kintner, C.R. (1986). Glilial growth factor and nerve-dependent proliferation in the regeneration blastema of urodele amphibians. *Cell* **45**: 301-306.

Brockes, J.P. (1989). Retinoids, homeobox genes and limb morphogenesis. *Neuron* **2**: 1285-1294.

Carlone, R.L. and Mescher, A.L. (1985). Trophic factors from nerves. In *Regulation of Vertebrate Limb Regeneration* (Sicard, R.E., ed.), pp. 93-103. Oxford University Press, New York.

Evans, R.M. (1988). The steroid and thyroid hormone receptor superfamily. *Science* **240**: 889-895.

Giguere, V., Ong, E.S., Sequi, P. and Evans, R.M. (1987). Identification of a receptor for the morphogen retinoic acid. *Nature* **330**: 624-629.

Giguere, V., Ong, E.S., Evans, R.M. and Tabin, C.J. (1989). Spatial and temporal expression of the retinoic acid receptor in the regenerating newt limb. *Nature* **337:** 566-569.

Globus, M. (1978). Neurotrophic contribution to a proposed tripartate control of the mitotic cycle in the regeneration blastema of the newt, *Notophthalmus (Triturus) viridescens*. *Amer. Zool.* **18**: 855-868.

Globus, M. and Alles, P. (1990). A search for immunoreactive substance P and other neural peptides in the limb regenerate of the newt *Notophthalmus viridescens*. *J. Exp. Zoo.* 254: 165-176.

Goss, R.J. (1969). Principles of Regeneration. Academic Press Inc., New York.

Gospodarowicz, D. (1974). Localisation of a fibroblast growth factor and its effect alone and with hydrocortisone on 3T3 cell growth. *Nature* **249**: 123.

Inten, L. and Bryant, S.V. (1973). Forelimb regeneration from different levels of amputation in the newt, *Notopthalmus viridescens*: Length, rate and stages. *Wilhelm Roux' Archiv.* **173**: 263-282.

Jabaily, J.A. and Singer, M. (1977). Neurotrophic stimulation of DNA synthesis in the regenerating forelimb of the newt, *Triturus*. *J. Exp. Zool.* **199**: 251-256.

Kemmner, W. and Schaller, H.C. (1984). Actions of head activator and head inhibitor during regeneration in hydra. *Differentiation* **26**: 91-96.

Lebowitz, P. and Singer, M. (1970). Neurotrophic control of protein synthesis in the regenerating limb of the newt, *Triturus*. *Nature* **225**: 824-827.

Liversage, R.A. (1987). Limb regeneration in vertebrates: regulatory factors. *Biochem. Cell Biol.* **65**: 726-729.

Liversage, R.A., McLaughlin, D.S and McLaughlin, H.M.G. (1985). The hormonal milieu in amphibian appendage regeneration. In *Regulation of Vertebrate Limb Regeneration* (Sicard, R.E., ed.), pp. 54-80. Oxford University Press, New York.

Liversage, R.A. and Globus, M. (1977). *In vitro* regulation of innervated forelimbs explants of *Ambystoma* larvae. *Can. J. Zool.* **55**: 1195-1199.

Maden, M. (1982). Vitamin A and pattern formation in the regenerating limb. *Nature* **295**: 672-675.

Mescher, A.L. and Loh, J.J. (1981). Newt forelimb regeneration blastemas *in vitro*: cellular response to explanation and effect of various growth substances. *J. Exp. Zool.* **216**: 235-245.

Petkovich, M., Brand, N.J., Kurst, K. and Chambon, P. (1987). A human retinoic acid receptor which belongs to the family of nuclear receptors. *Nature* **330**: 444-450.

Raff, M.C., Abney, E. Brockes, J.P., and Hornby-Smith, A. (1978). Schwann cell growth factors. *Cell* **15**, 813-822.

Rozengurt, E. and Sinnett-Smith, J. (1983). Bombesin stimulation of DNA and cell division in cultures of Swiss 3T3 cells. *Proc. Natl. Acad. Sci. USA* **80**: 2936-2940.

Schaller, H.C., Hoffmeister, A.H. and Dübel, S. (1989a). Role of the neuropeptide head activator for growth and development in hydra and mammals. *Development [Suppl]* **107:** 99-107.

Schaller, H.C., Druffel-Augusin, S., and Dübel, S. (1989b). Head activator acts as an autocrine growth factor for NH15-CA2 cells in the G2/mitosis transition. *EMBO J.* **8(11)**: 3311-3318.

Schaller, H.C., Roberge, M., Zachmann, B., Hoffmeister, S., Schilling, E., and Bodenmüller, H. (1986). The head activator is released from regenerating hydra bound to a carrier molecule. *EMBO J.* **5(8)**: 1821-1824.

Schaller, H.C. and Bodenmüller, H. (1985). Role of the neuropeptide head activator for nerve function and development. *Biol. Chem. Hoppe-Seyler* **366**: 1003-1007.

Schaller, H.C. and Bodenmüller, H. (1981). Isolation and amino acid sequence of a morphogenetic peptide from hydra. *Proc. Natl. Acad. Sci. USA* **78(11)**: 7000-7004.

Singer, M. (1952). The influence of the nerve in regeneration of the amphibian extremity. *Quart. Rev. Biol.* **27**: 169-200.

Singer, M. (1974). Neurotrophic control of limb regeneration in the newt. *Ann. N.Y. Acad. Sci.* **228:** 308-321.

Singer, M. (1978). On the nature of the neurotrophic phenomena in urodele limb regeneration. *Amer. Zool.* **18:** 829-841.

Spallanzani, L. (1769). An essay on animal reproductions. T. Becket, London (Translated from Italian by M. Maty).

Stocum, D.L. (1985). The role of the skin in urodele limb regeneration. In *Regulation of Vertebrate Limb Regeneration* (Sicard, R.E., ed.), pp. 32-52. Oxford University Press, New York.

Stocum, D.L. (1984). The urodele limb regeneration blastema, determination and organization of the morphogenetic field. *Differentiation* **27**: 13-28.

Tank, P.W., Carlson, B.M. and Connelly, T.G. (1976). A staging system for forelimb regeneration in the axolotl, *Ambystoma mexicanum*. *J. Morph.* **150**: 117-128.

Tassava, R.A. , Goldhamer, D.J., and Tomlinson, B.L. (1987). Cell cycle controls and the role of nerves and the regenerate epithelium in urodele forelimb regeneration: possible modifications of basic concepts. *Biochem. Cell Biol.* **65**: 739-749.

Tassava, R.A. and Olsen, C.L. (1985). Neurotrophic influences on cellular proliferation in urodele imb regeneration: *in vivo experiments*. In *Regulation of Vertebrate Limb Regeneration* (Sicard, R.E., ed.), pp. 81-91. Oxford University Press, New York.

Thomas, S.D. and Stocum, D.L. (1984). Retinoic acid-induced pattern duplication in regenerating urodele limbs. *Dev. Biol.* **103**: 319-328.

Todd, T.J. (1823). On the process of reproductionof the members of the aquatic salamander. *Quart. J. Sci.* **16**: 84-96.

Tsonis, P.A. (1991). Amphibian limb regeneration. *in vivo* **5**: 541-550.

Vethamany-Globus, S. (1987). Hormone action in newt limb regeneration: insulin and endorphins. *Biochem. Cell Biol.* **65**: 730-738.

Wanek, N., Gardiner, D.M., Muneoka, K. and Bryant, S.V. (1991). Conversion by retinoic acid of anterior cells into ZPA cells in the chick wing bud. *Nature* **350**: 81-83.

Washabaugh, C.H. and Tsonis, P.A. (1992). Histological analysis of forelimb regeneration in the California newt *Taricha granulosa*. *in vivo* **6**: 129-134.

Westall, F.C., Lennon, V.A., and Gospodarowicz, D. (1978). Brain derived fibroblast growth factor: identity with a fragment of the basic protein of myelin. *Proc. Natl. Acad. Sci. USA* **76**: 4675-4678.

CHAPTER 2.

Expression of Hydra Head Activator in Newt Tissues and Effects on Limb Regeneration

Abstract

In this study, the presence of the hydra head activator (HHA) neuropeptide and its influence on regenerating newt limbs (*Notophthalmus viridescens*) was investigated. Immunohistological analysis has localized the HHA neuropeptide in the adult newt brain, eye, intestine, and regenerating blastema. Experiments in which 9 day limb regenerates were denervated and subsequently implanted with HHA-soaked beads suggest a slight progression of blastema growth compared to denervated controls.

Introduction

The adult newt, *Notophthalmus viridescens*, is widely known for its ability to regenerate an injured or surgically amputated limb. Initially, epidermal cells migrate from the periphery of the wound producing an apical epidermal layer. This wound epithelium is crucial to the regenerative process; in its absence, limb regeneration does not proceed. As limb regeneration continues, differentiated cells such as muscle and cartilage dedifferentiate into embryonic-like mesenchymal cells. These cells, known as blastema cells, proliferate and begin to accumulate beneath the wound epithelium. Eventually, the blastema cells re-differentiate into the new cartilage and bone cells of the regenerating limb. Finally, morphogenesis will ensue replacing any missing structures of the amputated limb (Goss, 1969; Tsonis,1991).

The nerve-dependence in newt limb regeneration has been well documented (Singer, 1952). It has been shown that adequate innervation is necessary for proper limb regeneration and that a completely denervated limb will not regenerate. However, this nerve- dependence of the limb blastema is required only during the first 17 days post-amputation. Once a nerve-dependent blastema has been deprived of its nerve supply, it ceases to grow and is subsequently resorbed. In contrast, a nerve-independent blastema (blastema older than $\approx$ 17 days) is able to re-

differentiate and morphogenesis can lead to a regenerated limb (Singer and Craven, 1948).

On the molecular level, denervation of the limb blastema results in the reduction of protein, RNA, and DNA synthesis. Tassava and colleagues have shown that in the absence of nerves, dedifferentiation of stump cells does occur along with DNA synthesis, but cell division is arrested (Tassava, 1978; Mescher, 1982). In contrast, Maden (1978) has proposed that nerve fibers influence either the total number of blastema cells cycling or the rate at which they cycle by varying the length of the G_1 phase. Tassava et al. (1987) suggest that the blastema cell cycle is a "punctuated" phenomena whereby cells are constantly alternating between active cycling and transient quiescence. In any case, it seems that adequate innervation may provide cues which allow arrested cells to continue cycling and hence advance the proliferation of the blastema.

The reliance of the early blastema upon adequate innervation has been described by Singer (1952) as a neurotrophic phenomenon. This neurotrophic phenomena is hypothesized to originate in nerve fibers and postulated to promote blastema cell proliferation. Although the identity of this neurotrophic "factor(s)" remains unknown, several candidate molecules have been investigated (Carlone and Mescher, 1985; Brockes, 1984). Furthermore, several lines of evidence strongly suggest the neurotrophic "factor" is a protein or peptide molecule (Singer et al., 1976). Separate studies have implicated divalent calcium (Foret, 1973), cyclic nucleotides (cAMP and cGMP) (Globus et al., 1987), and inositol phosphates (Tsonis,

1991) as mediators of this neurotrophic effect. Recently, Globus and Alles (1990) investigated the presence of several neuropeptides such as substance P, neurotensin, and bombesin in the regenerating limb blastema, however their specific roles in regeneration were not detailed.

In hydra, a neuropeptide is responsible for head-specific growth and differentiation of epithelial and interstitial cells (Schaller et al., 1989a). This neuropeptide, the hydra head activator (HHA) was first isolated from the freshwater *Cnidaria, Hydra vulgaris* (formerly *Hydra attenuata*) (Schaller and Bodenmüller, 1981). Subsequent studies have revealed its presence and conserved amino acid sequence (pGlu-Pro-Pro-Gly-Gly-Ser-Lys-Val-Ile-Leu-Phe) in many species including mammals (Bodenmüller and Schaller, 1981).

In addition to HHA's conserved sequence, there is evidence that its growth-controlling function may also be preserved. In developing rat embryos, the expression of HHA appears early in the brain and intestine, lasting throughout development (Schaller et al., 1977). The HHA has been found in tumors and tumor cell lines of neural and endocrine origin (Schaller et al., 1988). In neuroblastoma cell lines, cellular growth is dependent upon the neuropeptide where it acts as an autocrine growth factor at the G_2/mitosis transition (Schaller et al., 1989b). Kajiwara and Sato (1986) have shown that the HHA stimulates DNA, RNA, and protein synthesis in cultured chick embryo brain cells. This study also provides evidence that HHA induces an increase in cellular cAMP with concomitant decrease in cGMP. We have raised the possibility that the HHA may have an influential role in the

regenerating newt limb. In this study, the presence of the HHA neuropeptide and its ability to promote blastema proliferation was investigated.

Materials and Methods

Animals and surgical techniques

Adult newts, *Notophthalmus viridescens*, were obtained from Charles Sullivan Co., Nashville, Tennessee were maintained in treated tap water at 21-25°C and fed raw chicken or beef liver two or three times weekly. Prior to all surgical procedures, animals were anesthetized with 0.01% phosphate-buffered aminobenzoic acid ethyl ether at pH 7 (Sigma Chemical Co.). Forelimb amputations were bilateral at the mid-radius/ulna level. Left forelimbs were denervated using fine forceps by severing the brachial nerves distal to the brachial plexus (Goldhamer and Tassava, 1987). The success of denervation was demonstrated by lack of limb movement and lack of response to sensory stimulation. Bead implantations were performed on ten-day limb regenerates using a fine, glass microinjection needle. In each case, approximately 4-5 beads were implanted into the blastema through the wound epidermis. Control limbs were punctured and received no implant beads. Previous studies have determined that beads alone have no effect on the limb regenerate (our previous studies, Wanek et al., 1991).

Immunohistochemistry

Adult newts were amputated as previously stated. At one or two weeks post-amputation, limbs and tissue specimens were excised and immediately frozen in O.C.T. compound (Miles, Elkhart, IN). Cryostat sections were cut longitudinally between 6 and 8μm along the anterior-posterior axis and placed on precleaned slides.

The primary antibody to the HHA neuropeptide (code K-8303) was raised in rabbit (Ekman et al., 1990) and diluted 1:50 with phosphate-buffered saline (PBS). Prior to staining, all sections were rehydrated using PBS containing 5% goat serum albumin. Primary staining was visualized using a 1:20 dilution of IgG fluorescein isothiocyanate (FITC)-conjugated goat anti-rabbit antiserum (Sigma Chemical Co.).

Preparation of bead implants

HHA neuropeptide (Sigma Chemical Co.) was monomerized at a concentration of 0.45mM using 3M ammonium sulfate as previously described (Bodenmüller et al., 1986). This stock solution was subsequently diluted to 13.4μM (0.017mg ml^{-1}) with 1% BSA and 0.1M NaCl and used to completely saturate AG1-X4 basic anion exchange resin beads (Bio-Rad, 105-250 μm diameter) overnight at 4°C. These beads have been used in previous studies to slowly deliver hydrophobic retinoid molecules locally (Wanek et al., 1991). Assuming 100% adsorption by the beads, the maximum amount of peptide per bead would be approximately 3 μg.

Histological analysis

At appropriate times, experimental and control limbs were removed, fixed using Bouin's fixative and decalcified with 10% trichloroacetic acid. Treated limbs were imbedded in paraffin and sectioned longitudinally at 8-10μm. Sections from each limb were taken through a graded ethanol series and processed using Gomori's trichrome stain and hematoxylin. Brightfield microscopy was used for tissue section analysis.

Results and Discussion

Immunolocalization

The presence of the HHA neuropeptide in several species including mammals has been documented (Bodenmüller et al., 1981; ScMwller et al., 1977). In these studies, the peptide was either chemically extracted or detected by immunological assay in rat and human tissues. Specifically, significant amounts were found among the following tissues: intestine, eye and brain. Blood serum also contained the neuropeptide, and it was found at elevated levels in individuals with brain tumors (Schaller et al., 1988). Our results indicate the expression of the neuropeptide in adult newt tissues. Using polyclonal antisera and indirect fluorescence detection, the HHA immunoreactivity was evident in newt intestine, eye, limb blastema (Fig. 1), and brain (data not shown). Intestinal tissue demonstrated a high degree of fluorescence when exposed to HHA antisera (Fig 1b). Staining was cytoplasmic and most intense

on the lumenal epithelial layer. This tissues demonstrated the highest amount of immunoreactivity. The newt eye also displayed HHA immunoreactivity (Fig. 1c). Fluorescence patterns in the eye was strong for the outer corneal epithelial layer; only slight staining was evident for the interior corneal cells.

In addition to the above tissues, regenerating limbs (17 days post-amputation) were examined by immunofluorescence. Figure 1a shows distinct fluorescence in the apical epidermal layer of the limb regenerate. The intensity of staining was greatest on peripheral epidermal layers and diminished near the basal germative layer. Immunoreactivity was also evident in the mesenchymal cells, but at a lower level than found in the epidermis. These results are in agreement with previous studies of other, unrelated neuropeptides. Globus and Alles (1990) investigated several tachykinin (substance P, eledoisin, kassinin, substance K and neuromedin K) and non-tachykinin (bombesin, nerotensin, and net-enkephalin) neuropeptides. Of these, substance P yielded the strongest immunoreactivity displaying a similar staining pattern to that found with the HHA neuropeptide. An identical staining pattern was obtaiMwd for limb regenerates which were denervated as in Materials and Methods (data not shown). This result suggests the origin of the HHA is the limb itself, possibly the wound epithelium.

Limbs treated with exogenous HHA neuropeptide

Twenty-one adult newts were amputated bilaterally and allowed to regenerate nine days, at which time left forelimbs were denervated. On day ten, eleven

denervated limb regenerates were implanted with HHA-soaked beads. The innervated right limbs of each animal served as control for normal regeneration. The remaining ten animals were used as negative controls, representing denervation alone.

In general, denervated control limbs became arrested and did not progress further (Fig. 2b). Similar results have been reported extensively in the literature (Singer, 1952). No re-differentiation was evident and the density of blastema cells were noticeably reduced when compared to normal regenerates (Fig. 2a). Experimental limbs containing HHA-soaked beads, demonstrated a slight accumulation of blastema cells in 2/11 cases. As depicted in Fig. 2c, one can see an apparent increase in blastema cells in treated limb stumps, though not an accumulation as in normal regenerates. It could be that the HHA has a limited effect, but it does not seem to be sufficient as a neurotrophic factor. The presence of the HHA in the wound epithelium could argue for a signalling function in the regenerating limb, possibly via cyclic nucleotides. Further studies on the function(s) of the HHA and its receptor molecule could elucidate the specific functions of the neuropeptide on regenerative tissues other than hydra.

Figure 1. Hydra head activator immunoreactivity in newt tissues. (**A**) Normal 17-day newt regenerating limb blastema (we, wound epithelia; b, blastema cells), 75 X. (**B**) Newt intestinal tissue (l, lumen), 150 X. (**C**) Eye tissue (corneal epithelia), 150 X.

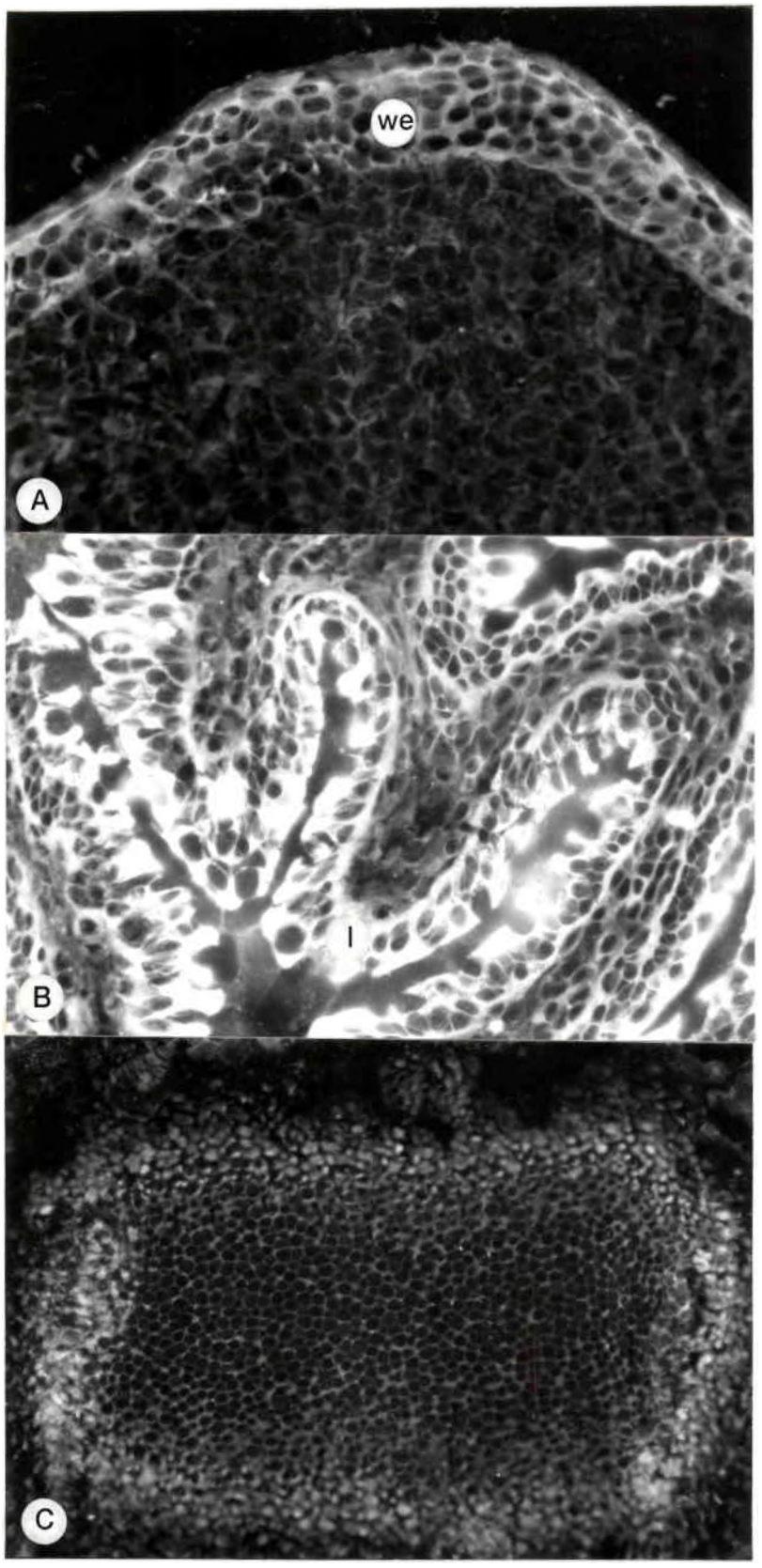
we
A
l
B
C

Figure 2. Effect of exogenous administration of the hydra head activator on regenerating newt limb blastema. In all figures, the dashed line represents the plane of amputation. The radius (r) and ulna (u) are depicted. Mesenchymal blastema cells (b) are labelled. Photographs were taken at 75 X. (**A**) A four-week normal, innervated regenerate displaying a full blastema and thick epidermal cap. (**B**) A four-week blastema which was denervated nine days after amputation. This blastema shows few mesenchymal cells and a thin epidermal cap. (**C**) This blastema was amputated and denervated as in (**B**). However, exogenous HHA was delivered locally (arrow) to the regenerate via a HHA-soaked bead. This regenerate displays a slight progression of blastema cells over (**B**), however it does not reach the size of normal regenerates (**A**).

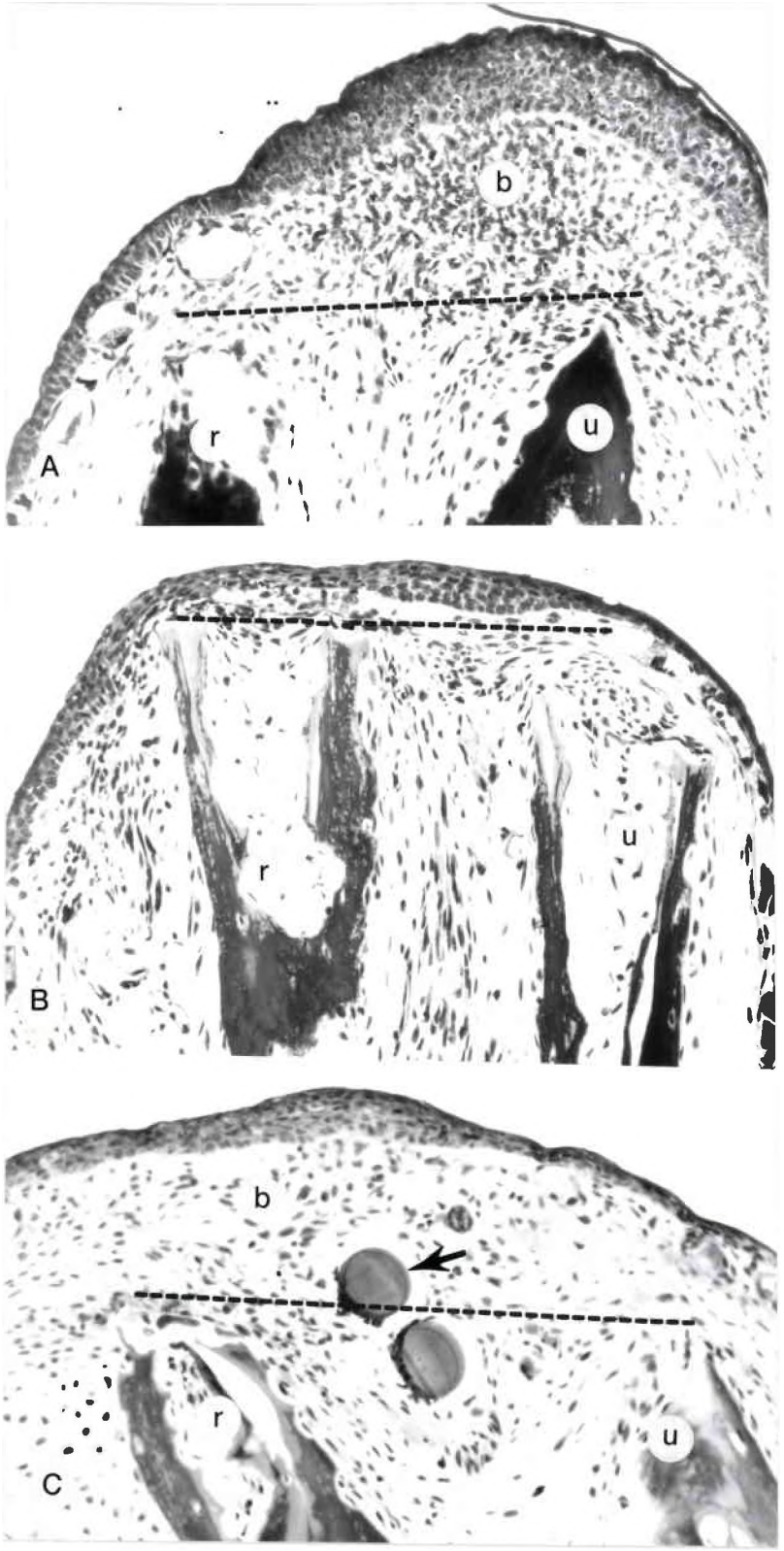
b
r
u
A
r
u
B
b
r
u
C

Literature Cited

Bodenmüller, H. and Schaller, H.C. (1981). Conserved amino acid sequence of a neuropeptide, the head activator, form coelenterates to humans. *Nature* **293:** 579-580.

Bodenmüller, H., Schilling, E., Zachmann, B. and Schaller, H.C. (1986). The neuropeptide head activator loses its biological activity by dimerization. *EMBO J.* **5(8):** 1825-1829.

Brockes, J.P. (1984). Mitogenic growth factors and nerve dependence on limb regeneration. *Science* **225:** 1280-1287.

Carlone, R.L. and Mescher, A.L. (1985). Trophic factors from nerves. In *Regulation of Vertebrate Limb Regeneration* (Sicard, R.E., ed.), pp. 93-103. Oxford University Press, New York.

Ekman, R., Salford, L., Brun, A., and Larsson, I. (1990). Hydra head activator-like immunoreactivity in human brain astrocytomas Grade III-IV and the surrounding brain tissue. *Peptides* **11:** 271-275.

Foret, J.E. and Babich, G.L. (1973) *Oncology* **28:** 83.

Globus, M., Vethamany-Globus, S., and Kesic, A. (1987). Control of blastema cell proliferation by possible interplay of calcium and cyclic nucleotides during newt limb regeneration. *Differentiation* **35:** 94-99.

Globus, M. and Alles, P. (1990). A search for immunoreactive substance P and other neural peptides in the limb regenerate of the newt *Notophthalmus viridescens*. *J. Exp. Zoo.* **254:** 165-176.

Goldhamer, D.L. and Tassava, R.A. (1987). An analysis of proliferative activity in innervated and denervated forelimb regenerates of the newt, *Notophthalmus viridescens*. *Development* **100:** 619-628.

Goss, R.J. (1969). Principles of Regeneration. Academic Press Inc., New York.

Kajiwara, S. and Sato, T. (1986). Growth promoting effect of head activator in cultured chick embryo brain cells. *Acta Endocrinologia* **113:** 604-608.

Maden, M. (1978). Neurotrophic control of the cell cycle during amphibian limb regeneration. *J. Embryol. Exp. Morph.* **48:** 169-175.

Mescher, A.L. (1982). Neurotrophic control of events in injured forelimbs of larval urodeles. *J. Embryol. Exp. Morph.* **69:** 183-192.

Schaller, H.C. and Bodenmüller, H. (1981). Isolation and amino acid sequence of a morphogenic peptide from hydra. *Proc. Natl. Acad. Sci. USA* **78(11):** 700-7004.

Schaller, H.C., Hoffmeister, A.H. and Dübel, S. (1989a). Role of the neuropeptide head activator for growth and development in hydra and mammals. *Development [Suppl]* **107:** 99-107.

Schaller, H.C., Druffel-Augustin, S., A.H. and Dübel, S. (1989b). Head activator acts as an autocrine growth factor for NH15-CA2 cells in the G_2/mitosis transition. *EMBO J.* **8(11):** 3311-3318.

Schaller, H.C., Schilling, L., Theilmann, H., Bodenmüller, H. and Sachsenheimer, W. (1988). Elevated levels of head activator in human brain tumors and in serum of patients with brain and other neurally derived tumors. *J. of Neuro-Oncology* **6:** 251-258.

Schaller, H.C., Flick, K. and Darai, G. (1977). A neurohormone from hydra is present in brain and intestine of rat embryos. *Neurochem.* **29:** 393-394.

Singer, M. (1952). The influence of the nerve in regeneration of the amphibian extremity. *Quart. Rev. Biol.* **27:** 169-200.

Singer, M. and Craven, L. (1948). The growth and morphogenesis of the regeneration forelimb of adult Triturus following denervation at various stages of development. *J. Exp. Zool.* **111:** 189-210.

Singer, M., Maier, C.E. and McNutt, W.S. (1976). Neurotrophic activity of brain extracts in forelimb regeneration of the Urodele, *Triturus*. *J. Exp. Zool.* **196:** 131-150.

Tassava, R.A. (1978). Neural control of cell cycle events in regenerating salamander limbs. *Amer. Zool.* **18:** 843-854.

Tassava, R.A., Goldhamer, D.J. and Tomlinson, B.L. (1987). Cell cycle controls and the role of nerves and the regenerate epithelium in urodele forelimb regeneration: possible modifications of basic concepts. *Biochem. Cell Biol.* **65:** 739-749.

Tsonis, P.A. (1991). Amphibian limb regeneration. *in vivo* **5:** 541-550.

Tsonis, P.A., English, D. and Mescher, A.L. (1991). Increased content of inositol phosphates in amputated limbs of axolotl larvae, and the effect of beryllium. *J. Exp. Zool.* **259:** 252-258.

Wanek, N., Gardiner, D.M., Muneoka, K. and Bryant, S.V. (1991). Conversion by retinoic acid of anterior cells into ZPA cells in the chick wing bud. *Nature* **350:** 81-83.

CHAPTER 3.

On the Three-dimensional Structure of the Hydra Head Activator Neuropeptide

Abstract

The structure of the Hydra head activator (HHA) neuropeptide has been previously studied using NMR, CD, and Raman spectroscopy and determined to contain between 62-67% anti-parallel β-pleated sheet, and predicted to assume a β-turn near the amino terminus. We have utilized spectroscopic data with the Double-Iterated Kalman Filter (DIKF) technique and CHARMm molecular mechanics to produce a molecular model of the HHA neuropeptide. Consistent with the secondary structure prediction, an anti-parallel β-pleated sheet topology was evident from the serine amino acid to the carboxyl terminus. Additionally, a β-turn occurred near the amino carboxyl terminus. Results indicate that fluctuations occurring at both termini may serve to stabilize the structure ultimately allowing the amino terminus access to its receptor protein.

Introduction

The Hydra head activator (HHA) neuropeptide was first isolated from the freshwater *Hydra attenuta* (Schaller and Bodenmüller, 1981). In hydra, this neuropeptide is required for the growth and differentiation of the head region (Schaller et al., 1990). Subsequent studies have revealed HHA's presence, with conserved amino acid sequence, in several species including mammals (Bodenmüller and Schaller, 1981). More recently, the HHA has been chemically extracted from mammalian tissues including rat and human brain, intestine, and blood serum (Schaller et al., 1977; Schaller et al., 1988). Additionally, tumor cell lines and patients having brain tumors have been shown to possess an abundance of the HHA, as have developing rat and human embryos (Schaller et al., 1989; Schaller et al., 1988). These findings suggest a role for the HHA in growth and development in mammals.

The primary sequence of the HHA neuropeptide has been determined as pGlu^{1}-Pro^{2}-Pro^{3}-Gly^{4}-Gly^{5}-Ser^{6}-Lys^{7}-Val^{8}-Ile^{9}-Leu^{10}-Phe^{11}, the amino terminus being pyroglutamic acid. This sequence displays little homology to other general sequences, although the bradykinins share a limited homology near the amino terminus (Xxx-Pro-Pro-Gly-Xxx-Ser). Interestingly, both peptides are able to stimulate ileum and uterus contraction (Schaller and Bodenmüller, 1981; Bodenmüller and Roberge, 1985). Immunological and biochemical studies have shown that the neuropeptide's

action is receptor mediated and biologically inactivated by self-aggregation (Schaller et al., 1988; Bodenmüller et al.,1986). Two receptors have been identified in the hydra which apparently mediate HHA's biological activity, possibly via cyclic nucleotides (Neubauer et al., 1991; Kajiwara and Sato, 1986). Knowledge of the HHA-receptor interactions is limited. However, amino acid mutation studies as well as immunological assays demonstrate a crucial role by amino-terminal residues for receptor binding and biological activity. In fact, cleavage of the $pGlu^1$ ring or its substitution by Tyr-Gln have resulted in biologically inactive peptides. Interestingly, alterations at the carboxyl terminal have also been effective in eliminating function (Birr et al., 1981).

Spectroscopic analysis and secondary structure prediction algorithms suggest a β-pleated conformation and a β-turn near the center of the neuropeptide. Specifically, experimental data from CD and Raman spectroscopy estimate between 62-67% β-pleated sheet in the anti-configuration (Bodenmüller et al.,1986). One and two-dimensional ^{1}H-NMR experiments have been performed and are consistent with this secondary structure data (Saffrich et al., 1989). No structural heterogeneity in the solution structure was evident, implying only one dominant conformation within the NMR time-scale. Assigned NOEs indicate a trans-configuration for the peptide bonds between residues $pGlu^1$, Pro^2, and Pro^3. Moreover, cleavage of the pyroglutamic ring did not induce any unexpected spectral modifications suggesting no

global conformational changes. Together, this spectroscopic data has provided secondary structure information, although no detailed three-dimensional model has been reported. It is the purpose of the present study to predict a general topology for the hydra head activator neuropeptide.

A few strategies have been developed to enable the incorporation of experimental data, e.g. distance constraints derived from NOEs, to Cartesian coordinate space in order to obtain a three-dimensional topology (Crippen, 1977; Havel et al., 1983). Recently, the PROTEAN methodology was introduced for protein solution structure determination. This method uses principles of Bayesian probability, namely the double-iterated Kalman filter procedure (DIKF), to sequentially refine estimates of the mean position and the variance of each atom. Thus a set of atomic positions consistent with the applied constraints, as well as an explicit quantification of the uncertainty in atomic position for each segment of the protein is provided (Altman and Jardetzky, 1989; Altman et al., 1989; Pachter et al., 1990). The technique was shown to perform well for deriving a structure from NMR data of the cyclic peptide Cyclosporin A (Pachter et al., 1992), the lac repressor headpiece (Altman et al., 1989), both the secondary structure (Arrowsmith et al., 1990) and tertiary structure of the trp repressor (Arrowsmith et al., 1991), and of the Kunitz inhibitor domain of the amyloid precursor protein involved in Alzheimer's disease (Batchelder, in prep.). In this study, we have used secondary structure data with the DIKF and CHARMm molecular dynamics modeling techniques to develop

and analyze a detailed three-dimensional fold of the hydra head activator neuropeptide.

Materials and Methods

Theory of double iterated Kalman filter

The structural model is described by the state vector **x** which consists of a list of the mean positions (x, y, z cartesian coordinates) for each of the atoms in the protein. The elements of the general error covariance matrix **C(x)** for any two atoms M, N are symmetric sub-matrices:

$$C(MN) = \begin{bmatrix} \sigma_{xMxN} & \sigma_{xMyN} & \sigma_{xMzN} \\ \sigma_{yMxN} & \sigma_{yMyN} & \sigma_{yMzN} \\ \sigma_{zMxN} & \sigma_{zMyN} & \sigma_{zMzN} \end{bmatrix}$$

The variance-covariance matrices on the diagonal of the covariance matrix [C(MM)] describe the extent of three-dimensional uncertainty in the position of the atom M. The sequence of distance or dihedral angle measurements **z** are represented by the appropriate non-linear function of the state vector **h(x)** and an assumed additive variance **v**. Stereochemical constraints such as the co-planarity of peptide bonds, aromatic rings and chirality are introduced by using suitable dihedral angles, or alternatively, the appropriately derived distances. Distance constraints also include covalent bond lengths, distances implied by bond angles, NOE distance constraints and any non-standard connectivities, for example, hydrogen bonds. Given this information, a sequential linear estimator for the minimum variance estimate of the

state can be obtained by utilizing the extended Kalman filter in the non-linear case (Gelb, 1984), originally introduced by Kalman (1960). This scheme is a conditional probability based (Bayesian) sequential estimation method, in which the experimental constraints **z** are compared with the corresponding values predicted from the estimated geometry of a given structure **x** and its variance-covariance **C(x)**, as well as from the measurement model **h(x)** and the variance **v** :

$$\mathbf{x}(+) = \mathbf{x}(-) + \mathbf{K}\{\mathbf{z} - \mathbf{h}(\mathbf{x}(-))\} \qquad [1]$$
$$\mathbf{C}(+) = \mathbf{C}(-) - \mathbf{K}\,\mathbf{H}\,\mathbf{C}(-)$$
$$\mathbf{K} = \mathbf{C}(-)\,\mathbf{H}^{\mathbf{T}}\{\mathbf{H}\,\mathbf{C}(-)\,\mathbf{H}^{\mathbf{T}} + \mathbf{v}\}^{-1}$$

where (-) signifies a previous (-) structural representation, which is sequentially updated (+). The rigorous criterion for the choice of the Kalman estimator gain matrix **K** is to minimize a weighted scalar sum of the diagonal elements of the error covariance matrix **C**. Moreover, there is an intuitive logic behind the equation for the magnitude of the adjustment **K**, namely, it can be seen as the "ratio" between the uncertainty in the estimate and that of the measurement. Particularly, if the variance of the experimental measurement is small relative to the variance of the predicted measurement as calculated from the current structural model, then the structure is updated to bring it into agreement with the experimental data. On the other hand, if the variance of the experimental measurement is large relative to the variance of the predicted measurement, then the structural model is updated only slightly to reflect the greater confidence in the structure than in the uncertain data information. The term within the inverse describes $\{\mathbf{C}(\mathbf{z}) = \mathbf{C}(\mathbf{h}(\mathbf{x})) + \mathbf{v}\}$ for the particular condition of a non-linear measurement model, since in the case of non-linearity,

$\mathbf{C(h(x))}$ corresponds to the first-order Taylor approximation of $\mathbf{h(x)}$, where $\mathbf{H}$ is the derivative of the data model, and $\mathbf{H}$ its transpose.

The extended Kalman filter approach can be used to obtain higher-order non-linear filters, and we adopted an iterative procedure for this purpose (Denham and Pines, 1966). The iterated extended Kalman filter for an iteration k is obtained by re-writing Eq. [1] :

$$\mathbf{x(+)}_k = \mathbf{x(-)} + \mathbf{K}_k \{\mathbf{z} - [\mathbf{h(x(+)}_{k-1}) + \mathbf{H(x(-)} - \mathbf{x(+)}_{k-1})]\} \qquad [2]$$

with similar expressions obtained for $\mathbf{C(+)}_k$ and the appropriate $\mathbf{K}_k$. This iterative procedure is carried out for each one of the constraints. However, since the filter is not optimal in the non-linear case, residual inaccuracies could still result. Thus, the final mean positions are used for another cycle (l) of updating. The covariance matrix is re-set to its initial large value in order to allow the atoms freedom to move in response to the constraints, and all measurements are re-introduced into the system for each of these doubly iterated cycles. These successive cycles are repeated until all constraints are satisfied to within a pre-set threshold of standard deviations.

The DIKF method is coded in the PROTEAN - Part II and was utilized in all computations (Altman et al., 1990). The algorithm updates the structural model (equation [2]) for a maximum of three iterations (k) for each of the distance constraints, with a threshold of 0.1 standard deviations for termination of the iterative procedure, while the number of cycles (l) for reaching convergence varies according to the experiment performed. In addition, at the end of each cycle all of the distance constraints are sorted according to the corresponding error evaluated from the

updated structure, so that the constraints with the worst errors are applied first in the next cycle.

Modeling of hydra head activator

The hydra head activator neuropeptide primary sequence was built using programs contained within PROTEAN - Part II. This sequence had a glutamine replacing the non-standard pyroglutamic residue. The input for the algorithm consisted of distance and angle constraints in the form of mean values along with associated variances. Specifically, distance variances were 0.1 $Å^2$ while angle variances remained at $25^{\circ 2}$. The amino terminal Gln^1, Pro^2 and Pro^3 ϕ_2, ψ_1 and ψ_2 angles were positioned at -55°, -60°, and +145°, respectively (Cantor and Schimmel, 1980). Furthermore, ten omega angles (C_α-C_α) were set at 180° of to retain a trans-configuration across the peptide bond. Based on spectroscopic data, ϕ and ψ backbone angles for Ser^6, Lys^7, Val^8, Ile^9 and ϕ of Leu^{10} were placed at average values for anti-parallel β-pleated sheet (ϕ = -139°, ψ = +135°) (Cantor and Schimmel, 1980). The aromatic ring of Phe^{11} was kept planar. Finally, 200 bond distances were assigned based on typical chemical bonding distances. In total, 228 angle and distance constraints were used as input to the structure determination computer algorithms coded in PROTEAN - Part II. This methodology allows a mean three-dimensional structure, consistent with experimental data, along with a variance and covariance of all atomic positions to be calculated.

Further refinement of the three-dimensional structure was carried out by performing molecular mechanics and dynamics calculations. Prior to modeling, all atom and bond types were verified and the amino-terminal glutamine was converted to pyroglutamic acid. The modeling protocol involved an initial energy minimization using the CHARMm force field energy function (Brooks et al., 1983) and subsequent integration of the classical Newtonian equation of motion to determine the position of atoms at later time points. The CHARMm force field energy function contained all default terms, excluding hydrogen bonding. In addition, a dielectric constant of unity and a time step of 5 femtoseconds was used for the dynamics simulations. Routinely, 10,000 steps of Steepest Descent (SD) energy minimization followed by Conjugate Gradient (CG) minimization were employed prior to molecular dynamics simulations. The neuropeptide was initially heated to 300 °K over a 5 ps span. Equilibration and simulation periods were performed at 300 °K for 5 ps and 50 ps, respectively. Over the 50 ps dynamics simulation, 1000 structures were written out for analysis. All computations were performed on a Cray X-MP and a Silicon Graphics Workstation.

Results

A three-dimensional fold for the hydra head activator neuropeptide was determined using experimental data derived from circular dichroism (CD) and nuclear magnetic resonance (NMR) in conjunction with theoretical techniques. After

being subjected to 40 cycles of the extended double iterated Kalman filter algorithm (DIKF), the average variance of the initial structure converged to less than 0.1 standard deviations (Figure 1). The mean position of the final structure from the DIKF calculation was subsequently used as a starting point for further refinement with molecular mechanics and dynamics.

The overall topology of the hydra head activator peptide is quite consistent with experimental data. Evident from the average dynamics structure (Figure 2 and Table I), the neuropeptide contains a β-turn near the mid-region. This bend allows for spatial proximity and bonding interactions between the amino and carboxyl termini. As seen in Table I, residues near the carboxyl terminus have ϕ and ψ torsion angles within the range for anti-parallel β-pleated sheet conformation, $\phi \approx -139^\circ$ and $\psi \approx +135^\circ$ (Cantor and Schimmel, 1980), while the amino terminus is less well defined.

The flexibility of the molecule is readily apparent by examining sequential coordinate frames of the dynamics simulation. However, a more quantitative measurement of flexibility can be seen in Figure 3, where the range of values for each ϕ and ψ torsion angle are plotted throughout the dynamics simulation. This plot emphasizes residues that demonstrate large fluctuations during the dynamics calculation. Transitions of 100° in the backbone angles are typical, though several residues show larger deviations. In particular, Pro^3, Gly^4, Gly^5, Ser^6 and Leu^{10} all display fluctuations near or over 200°. These residues represent regions of the neuropeptide having the most flexibility.

It is interesting to examine particular torsions as a function of elapsed time during the dynamics simulation. In Figure 4, such plots are given for pGlu[1], Pro[3], and Leu[10]. For comparison, Figure 4b depicts the trace of ϕ_3 over time and shows typical oscillations around an average torsion of -74°. Furthermore, no unique or repeating transitions are present suggesting little impact upon the overall structure. In contrast, traces of ψ_1, ψ_3 and ψ_{10} (Figure 4a, 4c and 4d, respectively) exhibit larger fluctuations in torsion values. The variation in ψ_1 and ψ_{10} is expected due to the inherent movement in unrestrained terminal residues. Their significance is underscored by mutational studies which indicate specific contacts between these residues are necessary for receptor binding and subsequent biological function (Birr et al., 1981; Schaller et al., 1989). Characteristic and repeating transitions are evident in ψ_3 (Figure 4c). These distinct transitions can be characterized by two specific structural features as seen in Figure 5. When ψ_3 is above +140°, a highly stabilized structure containing a β-turn is apparent (Figure 5a, 5b, and 5d). This model predicts extensive hydrogen bonding between residues comprising the β-turn. Indeed, residues Pro[3], Gly[4], Gly[5] and Ser[6] show hydrogen bonding (Table II). Figure 5c and 5e, represent a structure where hydrogen bonding between the amino and carboxyl termini occurs periodically. This structure is characterized by interactions between pGlu[1] and Val[8], Ile[9], Leu[10] and Phe[11] (Table II).

Discussion

The determination of the three-dimensional structure of small peptides poses a special challenge to the researcher largely due to the inherent flexibility of peptide molecules (Dyson and Wright, 1991). In lieu of crystallographic data or sufficient NMR interatomic distances, this challenge can be prohibitive. Thus, theoretical approaches such as molecular dynamics and other algorithms have become important for elucidation of structural and energetic aspects of peptides (Hagler et. al., 1985; Altman, 1990). Here, we have employed a methodology which incorporates readily available secondary structure data and a limited set of tertiary structural information into a molecular model.

In general, this strategy is computationally efficient and accurate as long as each stage in the course offers the next one a rigorous upper bound (Altman et al., 1989). This approach meets the major objections of Metzler et al. (1989) and Levy et al. (1989) to structure determination by distance geometry, since no structure is excluded from the system unless it does not satisfy the constraints. The estimates of mean and variance are updated using conservative constraint estimates one at a time, and there is no global optimization criteria which allows "error tradeoff" (a low average error at the expense of a few individually large errors). The resulting initial fold we calculated is therefore in good agreement with the experimental data.

The refined three-dimensional structure indicates that the neuropeptide contains a β-turn near the mid-region, which enables spatial proximity and interaction

between the termini. Moreover, the flexibility revealed in the structure, especially for unrestrained terminal residues, is significant. The importance of this point is emphasized by mutational studies which propose that specific contacts between these residues are important in receptor binding and biological function and inactivation by dimerization (Birr et al., 1981; Bodenmüller et al., 1986). In addition, the detailed molecular dynamics simulations enable us to discern interactions within the neuropeptide. Particularly, extensive hydrogen bonding is predicted between residues comprising the β-turn, as well a between the termini.

In Figure 6, a qualatative model of the dimerized peptide is presented, based on the model proposed by Bodenmüller et al. (1986). This model, depicts the anti-parallel orientation of two HHA molecules apparently stabilized by hydrophobic contacts between residues near the mid-region β-turn and hydrophobic carboxyl residues. Thus, one can imagine that by altering residues at either termini, crucial hydrogen bonding contacts can be disrupted important to biological function and dimerization.

In summary, in this study we have presented an analysis of the three-dimensional structure of the HHA neuropeptide. It is shown that the DIKF representation captures the relative uncertainty of the atomic positions in the peptide in a useful way for structural comparison, as well as for analysis for the flexible regions or those ill defined by the data. Further, molecular dynamics simulations provide insight into the specific interactions present in the peptide, for an understanding of its biological activity.

Figure 1. Average variance throughout DIKF calculation.

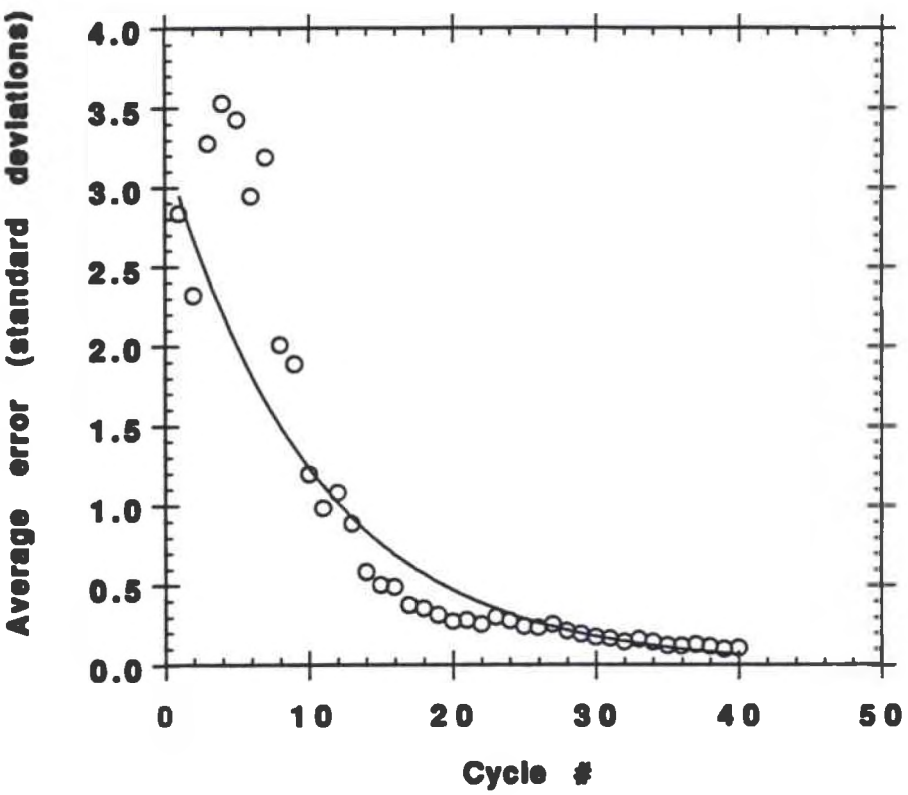
Average error (standard deviations)
4.0
3.5
3.0
2.5
2.0
1.5
1.0
0.5
0.0
0
10
20
30
40
50
Cycle #

Figure 2. Average structure of the Hydra head activator neuropeptide. The structure was generated from the average ϕ and ψ angles during the dynamics simulation.

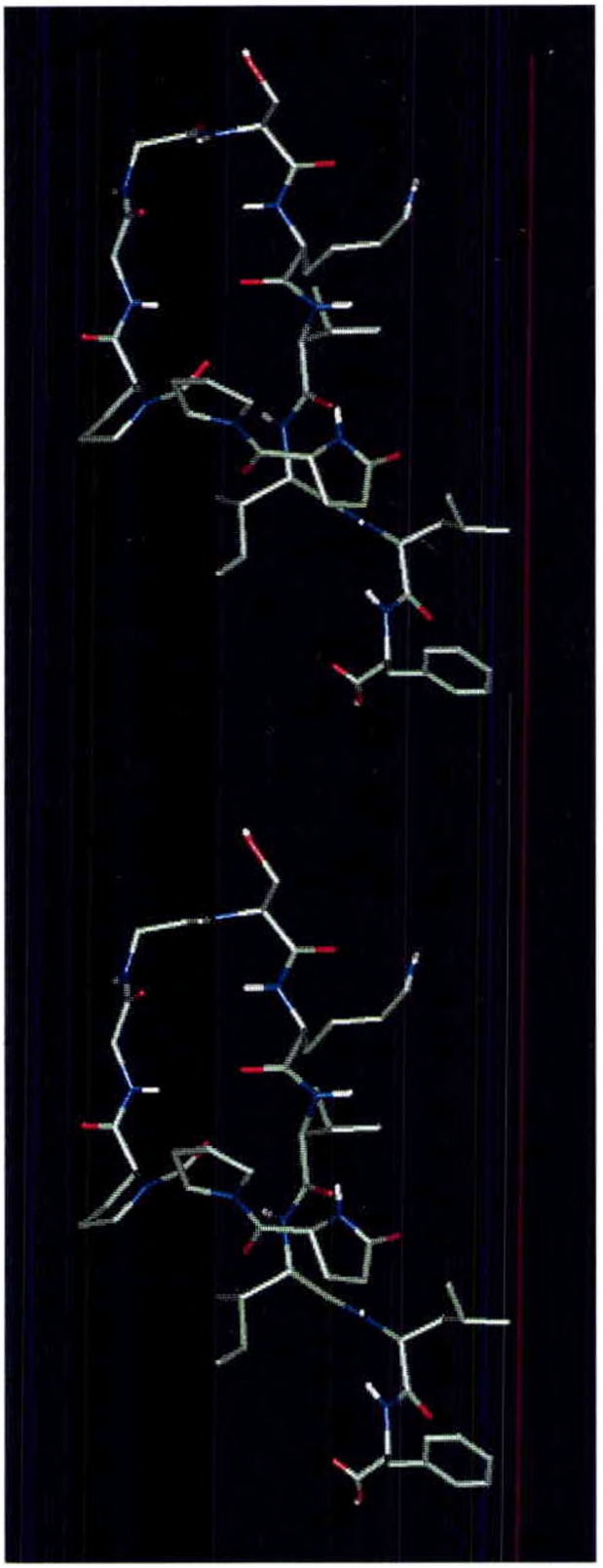

Figure 3. Plot of the accessible torsions (ϕ and ψ) sequentially along the backbone during 50 ps of dynamics simulation.

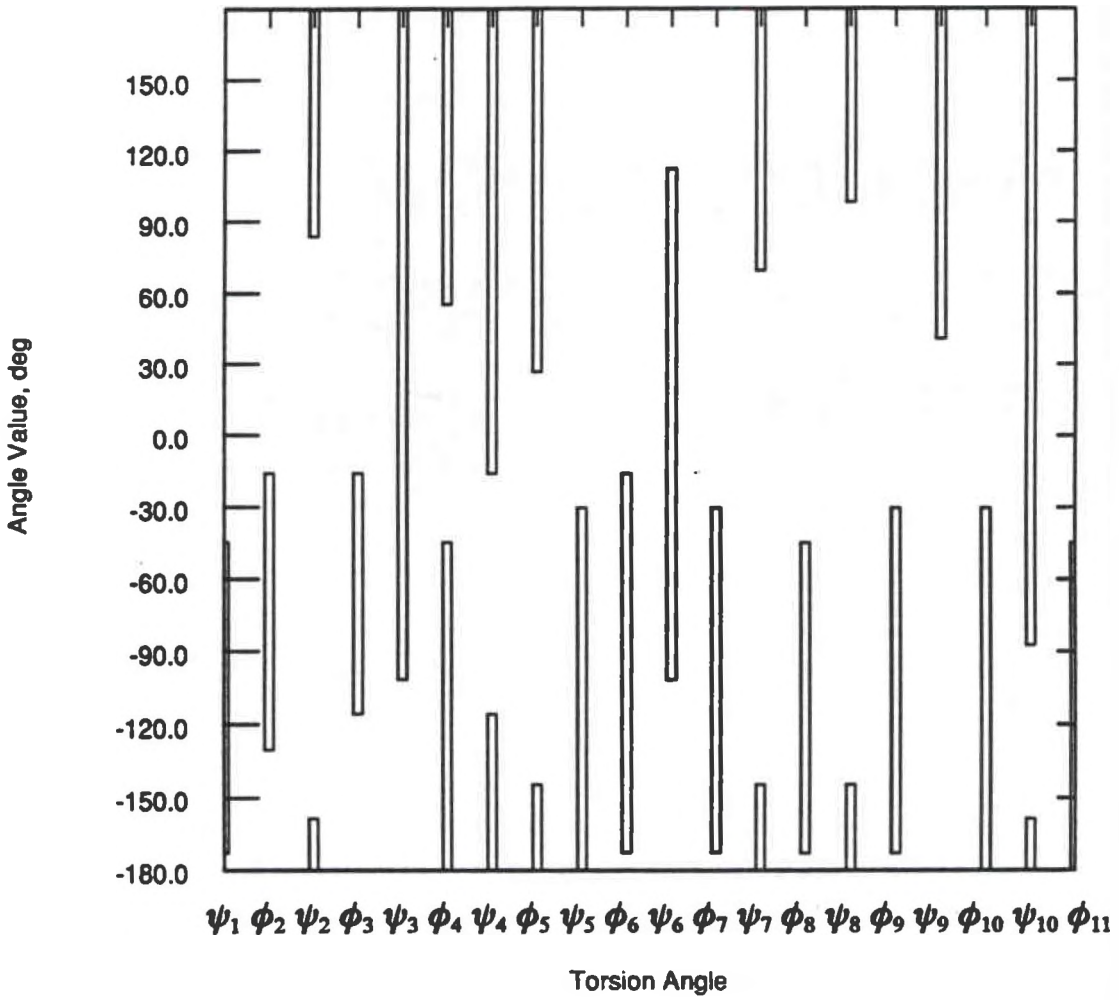
150.0
120.0
90.0
60.0
30.0
0.0
-30.0
-60.0
-90.0
-120.0
-150.0
-180.0
Angle Value, deg
ψ1 φ2 ψ2 φ3 ψ3 φ4 ψ4 φ5 ψ5 φ6 ψ6 φ7 ψ7 φ8 ψ8 φ9 ψ9 φ10 ψ10 φ11
Torsion Angle

Figure 4. Plot of the torsion angles ϕ and ψ as a functions of time elapsed during the dynamics simulation for ψ_1(a), ϕ_3(b), ψ_3(c) and ψ_{16}(d).

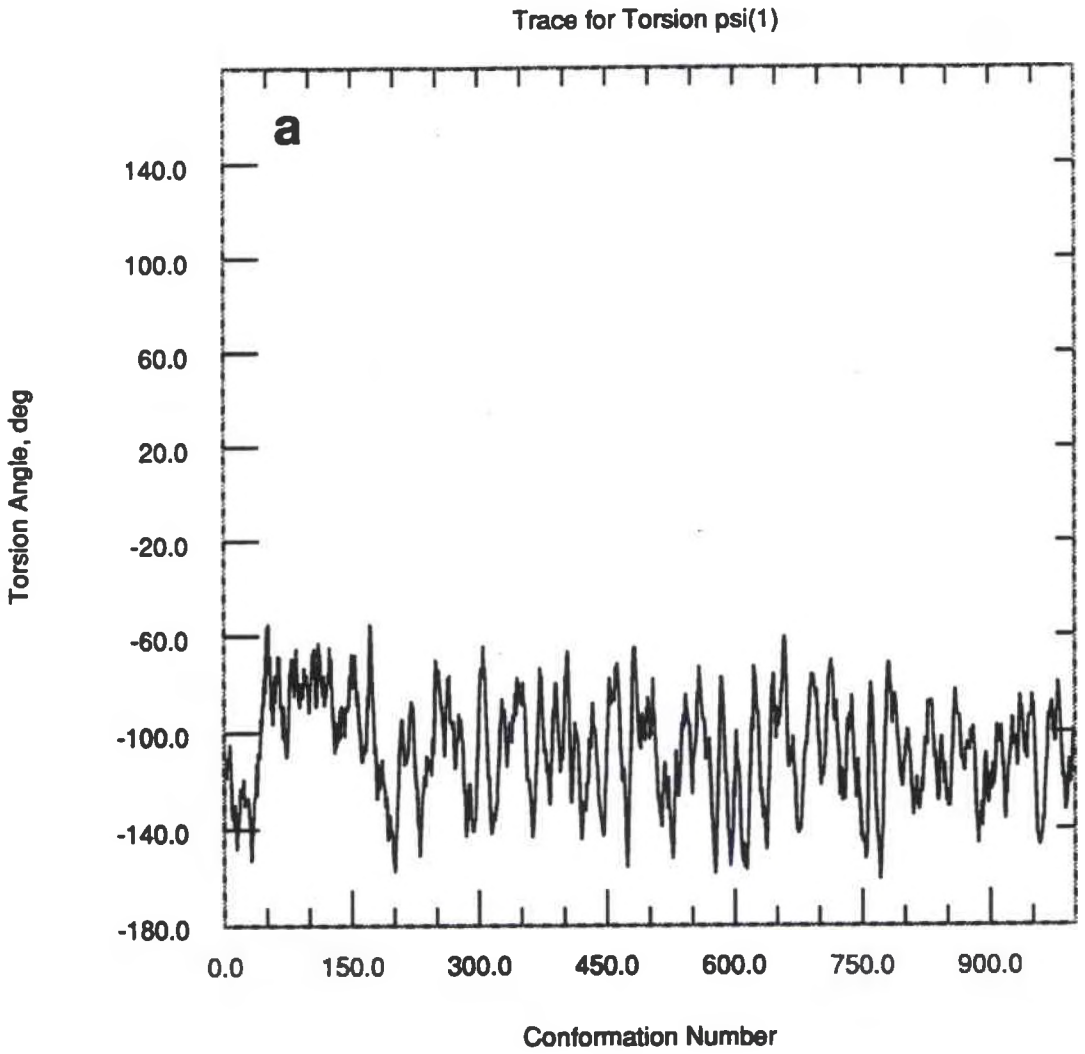
Trace for Torsion psi(1)
a
140.0
100.0
60.0
20.0
-20.0
-60.0
-100.0
-140.0
-180.0
Torsion Angle, deg
0.0
150.0
300.0
450.0
600.0
750.0
900.0
Conformation Number

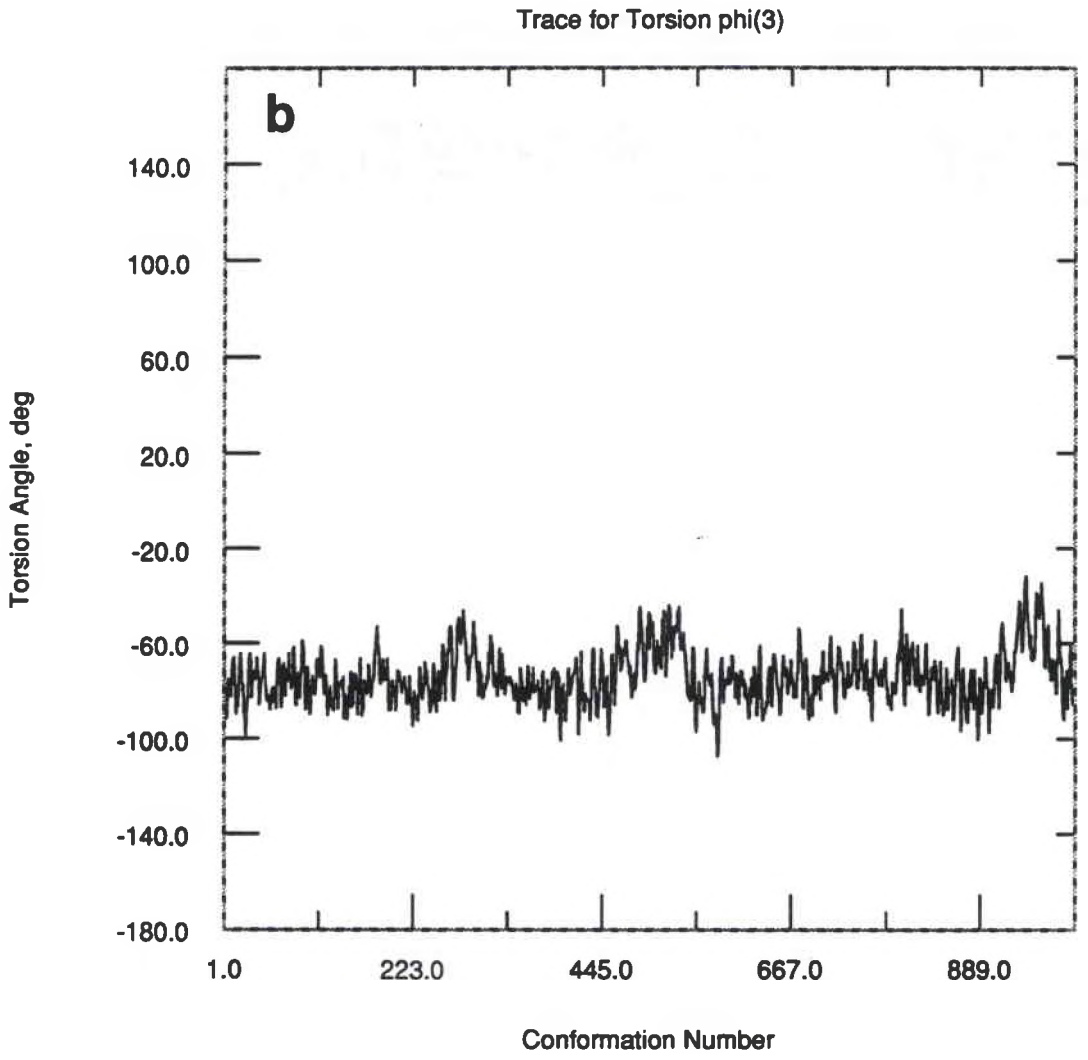
Trace for Torsion phi(3)
b
140.0
100.0
60.0
20.0
-20.0
-60.0
-100.0
-140.0
-180.0
Torsion Angle, deg
1.0
223.0
445.0
667.0
889.0
Conformation Number

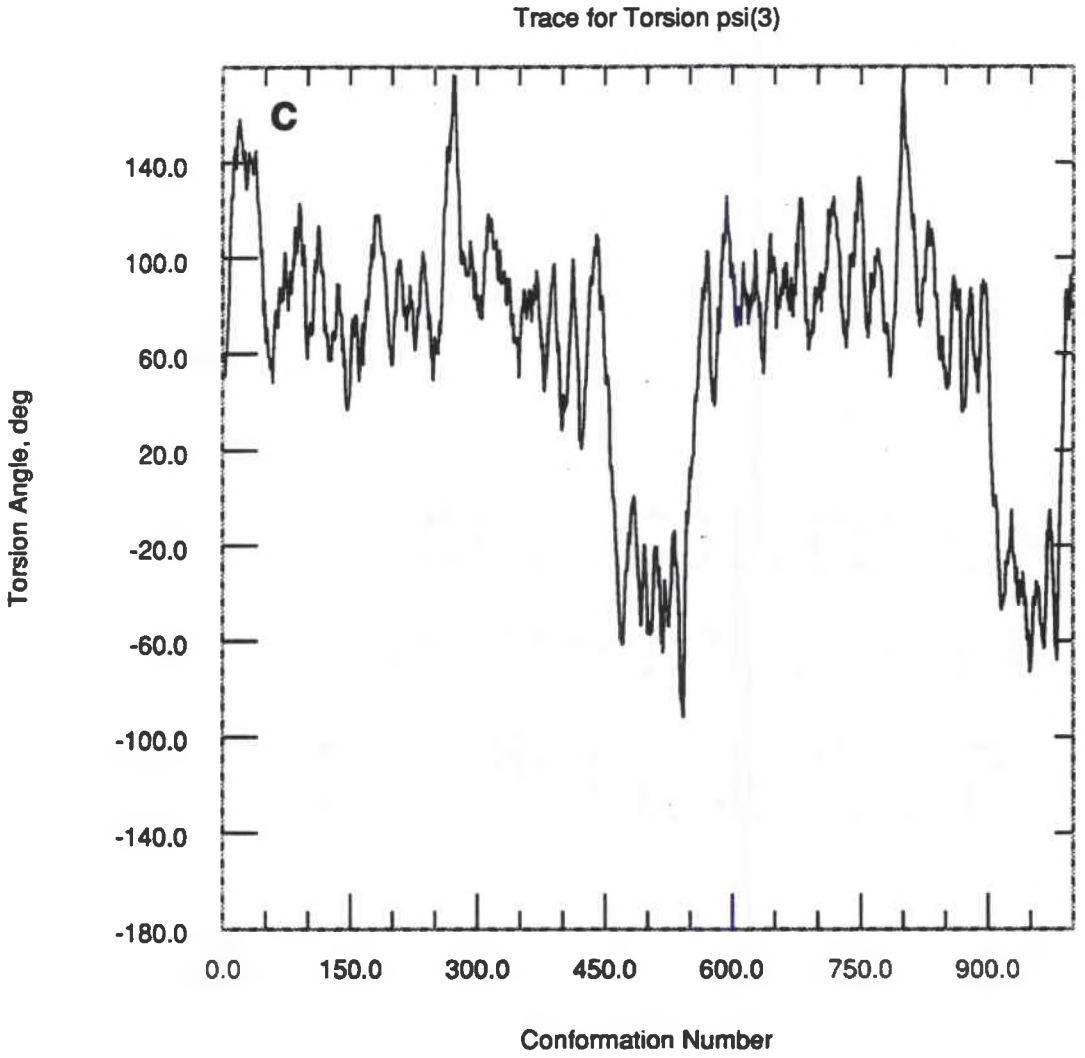
Trace for Torsion psi(3)
C
140.0
100.0
60.0
20.0
-20.0
-60.0
-100.0
-140.0
-180.0
0.0
150.0
300.0
450.0
600.0
750.0
900.0
Torsion Angle, deg
Conformation Number

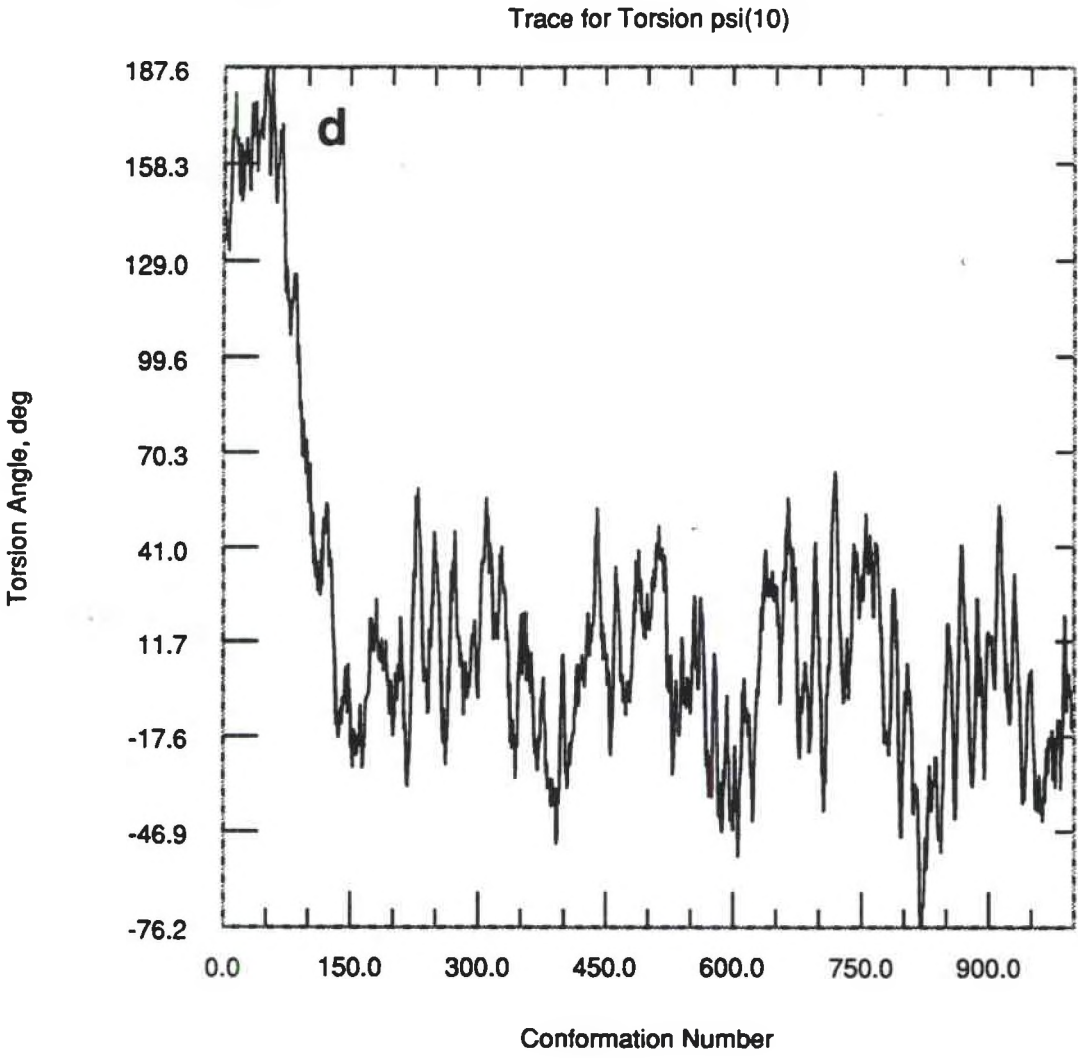
Trace for Torsion psi(10)
d
187.6
158.3
129.0
99.6
70.3
41.0
11.7
-17.6
-46.9
-76.2
Torsion Angle, deg
0.0
150.0
300.0
450.0
600.0
750.0
900.0
Conformation Number

Figure 5. Characteristic structural features apparent during trace of ψ_3 as a function of time.

c
b
a


ə
p

Figure 6. Proposed dimer structure of HHA neuropeptide.

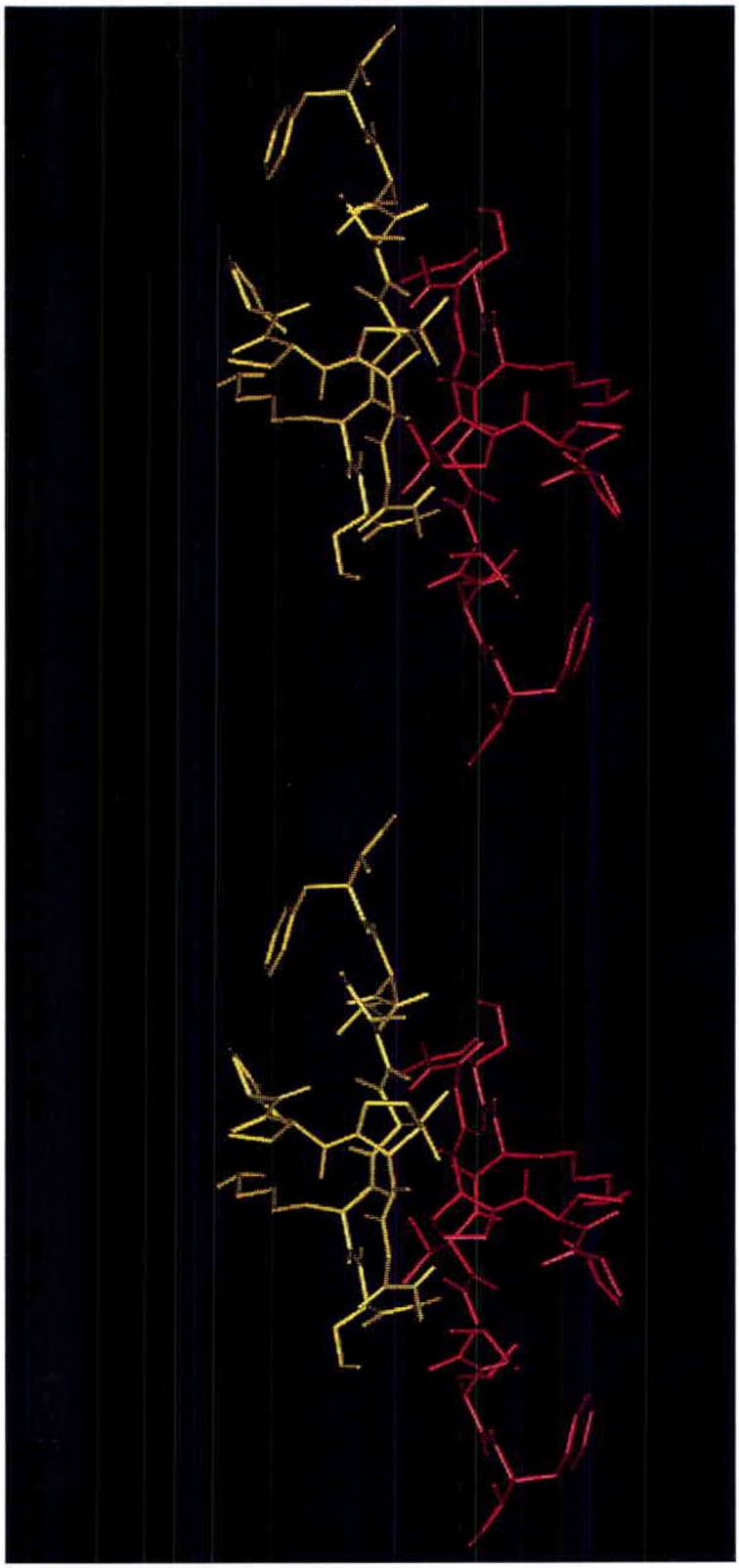

Table I. Average ϕ and ψ angles for the hydra head activator during 50 ps of dynamics simulation.

Residue	ϕ (deg)	ψ (deg)
pGlu[1]		- 107
Pro[2]	- 61	+ 138
Pro[3]	- 74	+ 64
Gly[4]	- 15	+ 59
Gly[5]	+ 89	- 103
Ser[6]	- 92	- 24
Lys[7]	- 107	+ 129
Val[8]	- 109	+ 114
Ile[9]	- 95	+ 123
Leu[10]	- 112	+ 15
Phe[11]	- 113	

Table II. Summary of hydrogen bonding during the dynamics simulation.

CO(pGlu[1])....NH(Lys[7])*
....NH(Leu[10])
....NH(Phe[11])
CO(Pro[2])....NH(Gly[4])
CO(Pro[3])....NH(Gly[5])
CO(Gly[4])....NH(Lys[7])
....NH(Ser[6])
CO(Ser[6])....NH(Lys[7])
....NH(Val[8])
CO(Lys[7])....NH(Gly[4])
CO(Val[8])....NH(pGlu[1])
....NH(Leu[10])
CO(Ile[9])....NH(Phe[11])
CO(Leu[10])....COOH(Phe[11])

* Signifies ϵ-amino of lysine side group.

Literature Cited

Altman, R.B. (1989) *Exclusion methods for the determination of protein structure from experimental data.* Ph.D. thesis, Medical Informations Sciences, Stanford University.

Altman, R.B. and Jardetzky, O. (1989) In *Methods in Enzymology* (Oppenheimer, N.J. and James, T.L., eds.), vol. 177, pp. 218-246. Academic Press Inc., New York.

Altman, R.B., Pachter, R. and Jardetzky, O. (1989) *Protein Structure and Engineering* (O. Jardetzky, ed.). Plenum Press, New York.

Altman, R.B., Pachter, R., Carrara, E.A. and Jardetzky, O. (1990) QCPE **X:4** 596.

Arrowsmith, C.H., Pachter, R., Altman, R.B., Iyer, S.B. and Jardetzky, O. (1990) Sequence-specific ^{1}H NMR assignments and secondary structure in solution of *Escherichia coli trp* repressor. *Biochemistry* **29:** 6322-6341.

Arrowsmith, C.H., Pachter, R., Altman, R.B. and Jardetzky, O. (1991) The solution structure of *E. Coli.* trp repressor and trp aporepressor at an intermediate resolution. *FEBS Eur. J. Biochem.* 202: 53.

Batchelder, L., Pachter, R., Jardetzky, O. and Cordell, B.L., in preperation.

Birr, C., Zachmann, B., Bodenmüller, H. and Schaller, H.C. (1981) Synthesis of a new neuropeptide, the head activator form hydra. *FEBS Lett.* **131(2):** 317-321.

Bodenmüller, H., Schilling, E., Zachmann, B. and Schaller, H.C. (1986) The neuropeptide head activator loses its biological activity by dimerization. *EMBO J.* **5(8):** 1825-1829.

Bodenmüller, H. and Schaller, H.C. (1981) Conserved amino acid sequence of a neuropeptide, the head activator, form coelenterates to humans. *Nature* **293:** 579-580.

Brooks, B.R., Bruccoleri, R.E., Olafson, B.D., States, D.J., Swaminathan, S. and Karplus, M. (1983) CHARMM: a program for macromolecular energy, minimization, and dynamics calculations. *J. Comp. Chem.* **4(2):** 187-217.

Cantor, C.R. and Schimmel, P.R. (1980) *Biophysical Chemistry*, Vol. I, W.H. Freeman Co., San Francisco.

Crippen, G.M. (1977) Rapid calculation of coordinates from distance matrices *J. Comp. Phys.* **26:** 449.

Denham, W.F. and Pines, S. (1966) *AIAA* **4:** 1071.

Dyson, H.J. and Wright, P.E. (1991) Defining solution conformations of small linear peptides. *Annu. Rev. Biophys. Chem.* **20:** 519-538.

Gelb, A. (1984) *Applied Optimal Estimation*, MIT Press.

Hagler, A.T., Osguthorpe, D.J., Dauber-Osguthorpe, P., and Hempel, J.C. (1985) Dynamics and conformational energetics of a peptide hormone: vasopressin. *Science* **227:** 1309-1315.

Havel, T.F., Kuntz, I.D. and Crippen, G.M. (1983) The theory and practice of distance geometry. *Bull. Math. Biol.* **45:** 665-720.

Kajiwara, S. and Sato, T. (1986) Growth promoting effect of head activator in cultured chick embryo brain cells. *Acta Endocrinologia* **113:** 604-608.

Kalman, R.E. (1960) Contributions to the theory of optimal control. *Bol. Soc. Mat. Mexicana* 102-119.

Levy, R.M., Bassalino, D.A., Kitchen, D.B. and Pardi, A. (1989) Solution structures of proteins form NMR data and modeling: alternative folds for neutrophil peptide. *Biochemistry* **28:** 9361-9372.

Metzler, W.J., Hare, D.R. and Pardi, A. (1989) Limited sampling of conformational space by the distance geometry algorithm: implications for structures generated from NMR data. *Biochemistry* **28:** 7045-7052.

Pachter, R., Altman, R.B., Czaplicki, J. and Jardetzky, O. (1991) The NMR solution structure of Cyclosporin A: comparison of structure determinations by the probability filtered estimate and other techniques. *J. Magn. Reson.* 92: 648.

Pachter, R., Altman, R.B. and Jardetzky, O. (1990) The dependence of a protein solution structure on the quality of the input NMR data. Application of the double-iterated Kalman filter technique to oxytocin. *J. Magn. Reson.* **89:** 578-584.

Saffrich, R., Kalbitzer, H.R., Bodenmüller, H., Muhn, P., Pipkorn, R. and Schaller, H.C. (1989) ^{1}H-nuclear magnetic resonance studies of the neuropeptide head activator. *Biochimica et Biophysica Acta* **997:** 144-153.

Schaller, H.C. and Bodenmüller, H. (1981) Isolation and amino acid sequence of a morphogenic peptide from hydra. *Proc. Natl. Acad. Sci. USA* **78(11):** 700-7004.

Schaller, H.C., Hoffmeister, A.H. and Dübel, S. (1989) Role of the neuropeptide head activator for growth and development in hydra and mammals. *Development [Suppl]* **107:** 99-107.

Schaller, H.C., Schilling, L., Theilmann, H., Bodenmüller, H. and Sachsenheimer, W. (1988) Elevated levels of head activator in human brain tumors and in serum of patients with brain and other neurally derived tumors. *J. Neuro-Oncology* **6:** 251-258.

Schaller, H.C., Flick, K. and Darai, G. (1977) A neurohormone from hydra is present in brain and intestine of rat embryos. *Neurochem.* **29:** 393-394.

Schaller, H.C., Druffel-Augustin, S., A.H. and Dübel, S. (1989) Head activator acts as an autocrine growth factor for NH15-CA2 cells in the G_2/mitosis transition. *EMBO J.* **8(11):** 3311-3318.